



Focal fatty sparing areas of the pediatric steatotic liver: pseudolesions on hepatobiliary phase magnetic resonance images

Gözde Özer
 H. Nursun Özcan
 Berna Oğuz
 Mithat Haliloğlu

Hacettepe University Faculty of Medicine,
Department of Radiology, Ankara, Türkiye

PURPOSE

Focal fatty sparing in liver can be detected as hyperintense pseudolesions on hepatobiliary phase magnetic resonance imaging (MRI). Distinguishing these pseudolesions from liver lesions may make diagnosis challenging. The aim of this study was to evaluate the imaging features of fatty sparing areas on liver MRI in pediatric patients who have been administered gadoxetate disodium.

METHODS

A total of 63 patients between January 2018 and June 2023 underwent gadoxetate disodium-enhanced liver MRI, and 9 (14%) patients with a focal fatty sparing were included in the study. The fat spared areas were evaluated qualitatively and quantitatively including signal intensity measurements and fat fraction calculations.

RESULTS

The liver MRI examinations of 9 patients (5 boys, 4 girls; aged 8–18 years, median age: 14.4) using gadoxetate disodium were evaluated. Based on in-phase and opposed-phase sequences, 13 areas of focal fatty sparing were identified. The mean fat fraction of the liver and fat spared areas were 26.2% (range, 15–47) and 9% (range, 2–17), respectively. All fat spared areas were hyperintense in the hepatobiliary phase images. The mean relative enhancement ratios of the liver and fat spared areas were 0.78 (range, 0.35–1.6) and 1.11 (range, 0.45–1.9), respectively.

CONCLUSION

Focal fatty sparing in liver in children was observed as hyperintense on hepatobiliary phase MRI, and it should not be identified as a focal liver lesion.

KEYWORDS

Liver, magnetic resonance imaging, gadoxetate disodium, hepatic steatosis, focal fatty sparing, children

Corresponding author: Gözde Özer

E-mail: gozdetufan@gmail.com

Received 19 August 2023; revision requested 20
September 2023; last revision received 22 September
2023; accepted 25 September 2023.



Epub: 30.11.2023

Publication date: 05.03.2024

DOI: 10.4274/dir.2023.232447

Non-alcoholic fatty liver disease has become common among children and includes a broad range of clinicopathologic features ranging from simple steatosis (fat without inflammation and/or fibrosis) and steatohepatitis/non-alcoholic steatohepatitis to cirrhosis.¹ Fatty liver in children can have various imaging manifestations, including diffuse and homogeneous, geographic, focal, and multifocal fat accumulation.² Focal areas of steatosis and fatty sparing in the liver can be detected as mass-like pseudolesions on ultrasonography or computed tomography (CT); in addition, these pseudolesions may show increased fluorodeoxyglucose (FDG) uptake on positron emission tomography (PET)/CT.³ Distinguishing these pseudolesions from metastases, particularly in pediatric patients with cancer, is crucial for preventing misdiagnosis. Liver magnetic resonance imaging (MRI) could be utilized as a problem-solving tool to assess focal liver lesions detected in a steatotic liver in both children and adults. Recently, the use of hepatobiliary contrast agents in children has become more common, and although these pseudolesions can be easily recognized with dual-echo imaging, hepatobiliary phase imaging may cause confusion because of metabolic alterations of liver parenchyma.

You may cite this article as: Özer G, Özcan HN, Oğuz B, Haliloğlu M. Focal fatty sparing areas of the pediatric steatotic liver: pseudolesions on hepatobiliary phase magnetic resonance images. *Diagn Interv Radiol.* 2024;30(2):135-138.

Focal fatty infiltration and fatty sparing in liver are well-known phenomenon in adults; however, in children, because of the low incidence of hepatic steatosis, these pseudolesions may make diagnosis challenging. The purpose of this study was to evaluate signal intensity (SI) features of fat spared areas on liver MRI in pediatric patients who have been administered gadoxetate disodium.

Methods

This retrospective study was approved by the Hacettepe University Non-Interventional Clinical Research Ethics Committee; informed patient consent was waived because the study was based on retrospective data analysis (GO 21/1162). The archive of the pediatric radiology unit was retrospectively reviewed for liver MRI examinations performed in our institution between January 2018 and June 2023. A total of 63 patients with indications of focal liver lesion, primary liver tumor, metastasis, and chronic liver disease underwent liver MRI with gadoxetate disodium administration. Patients with chronic parenchymal liver disease were excluded, and 9 patients with fat spared areas were included in the study. The MRI examinations were evaluated by two pediatric radiologists (H.N.O. and G.O.) with 11 and 2 years of experience, respectively, through consensus, using a picture archiving and communication system (PACS; GE Medical Systems, Milwaukee, WI, USA). The following clinical and radiological features were recorded: primary diagnosis, patients' age at the time of MRI, and fat spared areas and true lesions in the liver parenchyma on MRI. The fat spared areas were evaluated qualitatively and quantitatively. For the quantitative assessment of the fat fraction, a region of interest with an average size of 0.5 cm² was placed at the fat

spared areas and steatotic liver parenchyma on in-phase and opposed-phase images for SI measurements. The fat fraction was calculated according to the following formula: fat fraction = in-phase SI – opposed-phase SI / 2 × in-phase SI. The delta fat fraction was defined as the difference between the liver parenchyma and fat spared area. In addition, an SI measurement was also performed on precontrast fat-suppressed T1-weighted and hepatobiliary phase images at the liver parenchyma and fat spared areas. The relative enhancement ratio in the hepatobiliary phase images was calculated in both the liver parenchyma and fat spared areas using the following formula: (hepatobiliary phase SI) – (precontrast SI) / (precontrast SI).

The MRI examinations were performed using 1.5T MRI system (GE Signa HDx Healthcare, Milwaukee, WI, USA) units with an eight-channel phased-array body coil. The imaging protocol of the liver included breath-hold coronal TRUE-FISP [repetition time (TR), 4.3 ms; time to echo (TE), 2.1 ms; flip angle (FA), 60; matrix, 416 × 512; slice thickness, 4.5 mm], axial T2-weighted half-Fourier acquisition single-shot turbo spin-echo (TR, 1350 ms; TE, 92 ms; FA, 160; matrix, 256 × 256; slice thickness, 6 mm), axial in-phase and opposed-phase chemical shift imaging (TR, 160 ms; TE, in-phase: 4.9 ms, opposed-phase: 2.4 ms; FA, 70; matrix, 256 × 192; slice thickness, 6 mm), breath-hold T2-weighted fast spin-echo with fat suppression (TR, 3050 ms; TE, 125 ms; FA, 150; matrix, 256 × 256, slice thickness, 6 mm), and three-dimensional T1-weighted gradient-recalled echo fat-suppressed sequences (TR, 5 ms; TE, 2.4 ms; FA, 10; matrix, 320 × 240; slice thickness, 3 mm) before and after the injection of the contrast agent. A bolus injection of gadoxetate disodium (Primovist, Bayer HealthCare, Berlin, Germany) was administered at a rate of 1 mL/s. The total contrast dose was 0.1 mL/kg of body weight. Diffusion-weighted imaging

was used to acquire single-shot echo-planar images (under free-breathing) with *b* values of 50, 400, and 800 s/mm². The images were acquired in accordance with delayed hepatobiliary phase imaging at 20 min for gadoxetate disodium. Before the MRI examination, an informed consent form was obtained from the patients' parents regarding the use of gadoxetate disodium. Gadoxetate disodium is a widely used contrast agent in children and has been reported as safe in the literature.⁴

Results

Liver MRI examinations of 9 patients (5 boys, 4 girls; aged 8–18 years, median age: 14.4) using gadoxetate disodium were evaluated. The demographic characteristics are summarized in Table 1. None of the patients included in the study had liver cirrhosis.

A total of 13 focal fat spared areas were detected on in-phase and opposed-phase images (Table 2). On the opposed-phase images, the fat spared areas had high SI. The mean fat fraction of the liver and fat spared areas were 26.2% (range, 15–47) and 9% (range, 2–17), respectively. The median delta fat fraction was 15% (range, 12–34). The fat spared areas were hyperintense in 7 (78%) patients and isointense in 2 (22%) patients on fat-suppressed precontrast T1-weighted images (Figure 1). The mean SI of liver and fat spared areas on precontrast fat-suppressed T1-weighted images were 405 (range, 129–891) and 481 (range, 130–1277). The mean SI of liver and fat spared areas on hepatobiliary phase images were 736 (range, 175–1693) and 1112 (range, 203–2834). In the fat-suppressed T2-weighted images, the fat spared areas were hypointense in 5 (55%) patients and isointense in 4 (45%) patients. There was no signal alteration in any of the patients on the diffusion-weighted images. All the detected focal fat spared areas were hyperintense in the hepatobiliary phase images (Figure 1).

Main points

- Fatty liver disease has become more common in children in recent years.
- Focal fatty sparing can be detected as mass-like lesions on ultrasonography or computed tomography (CT) and may even show increased fluorodeoxyglucose uptake in positron emission tomography/CT.
- Liver magnetic resonance imaging with hepatobiliary contrast agents can be used as a problem-solving imaging modality in the evaluation of steatotic liver in children.
- Focal fat spared areas in the liver parenchyma may appear as increased signal intensity in the hepatobiliary phase, presumably because of the preserved parenchymal function.

Table 1. Demographic characteristics of the patients

Patient no	Age (years)	Sex	Primary diagnoses
1	13	M	Obesity, geographic liver lesion on abdominal ultrasound
2	11	F	Hodgkin lymphoma
3	18	M	Glycogen storage disease
4	16	F	Diabetes mellitus, PCOS, geographic liver lesion on abdominal ultrasound
5	8	F	Hypertriglyceridemia, liver lesion on abdominal ultrasound
6	17	M	Testicular yolk sac tumor
7	17	M	Hodgkin lymphoma
8	13	F	Glycogen storage disease
9	17	M	Hepatic adenoma

M, male; F, female; PCOS, polycystic ovary syndrome.

Table 2. Imaging findings of the patients

Patient no	Segments of FSAs	T2W fat-suppressed	T1W fat-suppressed	Arterial phase	Portal phase	Delayed phase	Hepatobiliary phase
1	Segment 7 and 8	Hypointense	Hyperintense	Hyperintense	Hyperintense	Hyperintense	Hyperintense
2	Segment 4 and 5	Isointense	Hyperintense	Hyperintense	Hyperintense	Hyperintense	Hyperintense
3	Segment 2 and 4	Hypointense	Hyperintense	Hyperintense	Hyperintense	Hyperintense	Hyperintense
4	Segment 3 and 4	Hypointense	Hyperintense	Hyperintense	Hyperintense	Hyperintense	Hyperintense
5	Segment 4	Isointense	Hyperintense	Hyperintense	Hyperintense	Hyperintense	Hyperintense
6	Segment 1 and 4	Hypointense	Hyperintense	Hyperintense	Hyperintense	Hyperintense	Hyperintense
7	Segment 4	Isointense	Isointense	Isointense	Hyperintense	Hyperintense	Hyperintense
8	Segment 3	Isointense	Isointense	Isointense	Hyperintense	Hyperintense	Hyperintense
9	Segment 4	Hypointense	Hyperintense	Hyperintense	Hyperintense	Hyperintense	Hyperintense

FSAs, fat spared areas.

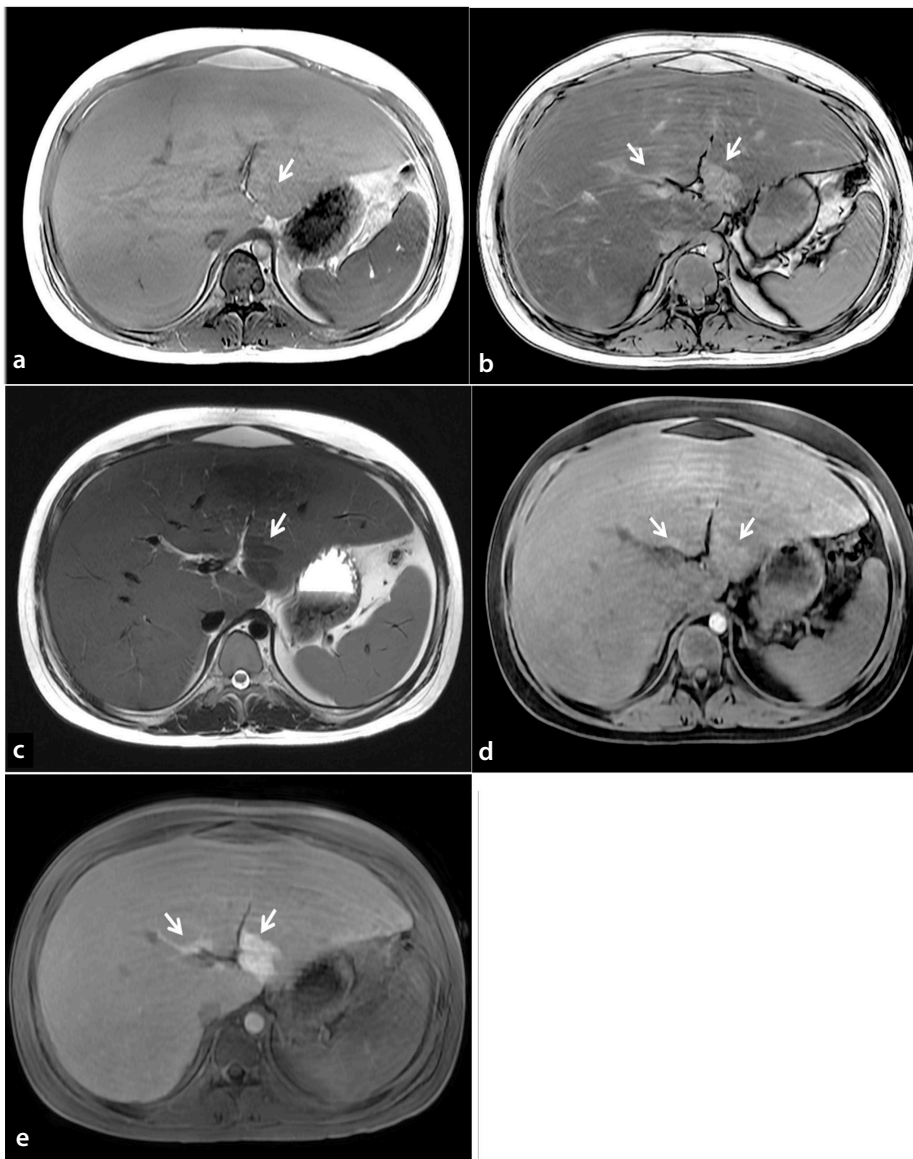


Figure 1. An 18-year-old boy with type 1 glycogen storage disease underwent liver magnetic resonance imaging using a hepatobiliary contrast agent. (a, b) In-phase (a) and opposed-phase (b) images indicating liver steatosis with decreased signal intensity on the opposed-phase image and fat spared areas in segments 2 and 4 (arrows). (c, d) Axial T2-weighted image indicating hypointensity (arrow), and precontrast fat-suppressed T1-weighted image displaying hyperintensity (arrow) at the focal fat spared area. (e) Hyperintensity at the focal fat spared area (arrows) on the hepatobiliary phase image 20 min after gadoxetate disodium injection.

The mean relative enhancement ratios of the liver and fat spared areas were 0.78 (range, 0.35–1.6) and 1.11 (range, 0.45–1.9), respectively. Fat spared areas were present at segment 1 (n = 1), segment 2 (n = 1), segment 3 (n = 2), segment 4 (n = 7), segment 5 (n = 1), segment 7 (n = 1), and segment 8 (n = 1). Five patients had a fat spared area in more than one liver segment.

Focal nodular hyperplasia was detected in 5 patients, and all of these lesions exhibited gadoxetate disodium retention in the hepatobiliary phase. One patient had histopathologically confirmed inflammatory hepatocellular adenoma that displayed wash-out on hepatobiliary phase images.

Discussion

This study produced two major results. First, focal fatty sparing in the pediatric steatotic liver demonstrates increased SI on hepatobiliary phase images. Second, we observed that most of these areas have increased SI on precontrast fat-suppressed T1-weighted images. On in-phase and opposed-phase images, fatty sparing has high SI on the opposed-phase images as a result of the suppressed signal of the other parts of the steatotic liver.

In our study, most of the fat spared areas were in segment 4. Some segments of the liver, such as the gallbladder fossa, medial segment of the left lobe adjacent to the portal vein, and subcapsular areas are more prone to focal fatty sparing.⁵ This phenomenon is caused by a third inflow, which is a venous inflow to the liver in addition to the typical dual blood supply (portal vein and hepatic artery). The most common anatomic variations that cause a third inflow are an aberrant right gastric vein, epigastric and para-umbilical veins (Sappey's and Burow's veins), and cholecystic veins.^{6,7} Focal fat spared ar-

areas are detected as focal hypoechoic areas on ultrasonography and hyperdense areas on CT, and these findings may be confused with solid liver lesions. MRI is considered the most reliable non-invasive diagnostic tool for evaluating hepatic steatosis.⁸ The dual-echo method can easily detect focal fat deposition or fatty sparing.

Hepatic steatosis leads to parenchymal inflammation and fibrosis and may cause decreased parenchymal function.^{9,10} Gadoxetate disodium-enhanced liver MRI can be used to evaluate the functional capacity of the liver parenchyma, and decreased enhancement on hepatobiliary phase images might be a sign of hepatocyte dysfunction caused by liver fibrosis and inflammation.^{11,12} Impaired hepatic function can be observed as decreased enhancement on hepatobiliary phase images.¹⁰ Therefore, focal fatty sparing can be observed as hyperintense pseudolesions on hepatobiliary phase images, presumably because of the preserved hepatocyte function. Ünal et al.¹³ reported similar findings in adult patients and suggested that fat spared areas demonstrating hyperintensity on hepatobiliary phase images may include hyperfunctioning hepatocytes compared with other parts of the liver. Fat spared areas of the liver may appear as focal areas of increased FDG uptake in FDG PET/CT.¹⁴⁻¹⁶ In addition, focal fat spared areas have been reported to mimic neuroendocrine tumor metastases in ⁶⁸Ga-Dotatate PET/CT.¹⁷ These reports may support the hypothesis of preserved or maybe even increased hepatocyte function in these areas.

In our study, 5 patients had focal nodular hyperplasia, which is an uncommon lesion in the pediatric population¹⁸ and has hyperintensity on hepatobiliary phase images; however, early arterial phase enhancement, persistent enhancement on delayed phases, and isointense to hyperintense signals on T2-weighted images might allow the differentiation of these lesions from fat spared areas.^{19,20} In addition, some subtypes of hepatocellular adenomas are observed as hyperintense on hepatobiliary phase images. In our study, 1 patient had an inflammatory hepatocellular adenoma that exhibited wash-out of the contrast media at 20 min. Inflammatory adenoma is the most common subtype related to oral contraceptives and obesity and may show contrast retention on hepatobiliary phase images.²¹ The fact that fatty liver is more common in these patients may make diagnosis challenging in liver MRI. Fatty sparing can be distinguished by the

strong enhancement of adenomas in the arterial phase.¹⁹

This study has several limitations. Our study group was small, and no histopathological correlation was identified in any patients. Biopsy was considered unnecessary because of the typical MRI findings and the benign nature of focal fatty sparing. The hyperintensity on hepatobiliary phase images may be secondary to precontrast T1 hyperintensity or hyperfunctional hepatocytes in fatty sparing areas.

In conclusion, liver steatosis may have various imaging manifestations in pediatric patients. Focal fat spared areas in children have been observed as hyperintense on hepatobiliary phase MRI, and they should not be identified as a focal liver lesion.

Conflict of interest disclosure

The authors declared no conflicts of interest.

References

- Schwimmer JB, Deutsch R, Kahen T, et al. Prevalence of fatty liver in children and adolescents. *Pediatrics*. 2006;118(4):1388-1393. [\[CrossRef\]](#)
- Özcan HN, Oğuz B, Haliloğlu M, Orhan D, Karçaaltıncaba M. Imaging patterns of fatty liver in pediatric patients. *Diagn Interv Radiol*. 2015;21(4):355-360. [\[CrossRef\]](#)
- Rydzak C, Chauhan A, Gupta N, Chuang HH, Rohren EM, Bhosale PR. Fat-containing hypermetabolic masses on FDG PET/CT: a spectrum of benign and malignant conditions. *AJR Am J Roentgenol*. 2016;207(5):1095-1104. [\[CrossRef\]](#)
- Ayyala RS, Anupindi SA, Gee MS, Trout AT, Callahan MJ. Intravenous gadolinium-based hepatocyte-specific contrast agents (HSCAs) for contrast-enhanced liver magnetic resonance imaging in pediatric patients: what the radiologist should know. *Pediatr Radiol*. 2019;49(10):1256-1268. [\[CrossRef\]](#)
- Tom WW, Yeh BM, Cheng JC, Qayyum A, Joe B, Coakley FV. Hepatic pseudotumor due to nodular fatty sparing: the diagnostic role of opposed-phase MRI. *AJR Am J Roentgenol*. 2004;183(3):721-724. [\[CrossRef\]](#)
- Yoshimitsu K, Honda H, Kuroiwa T, et al. Unusual hemodynamics and pseudolesions of the noncirrhotic liver at CT. *Radiographics*. 2001;21:81-96. [\[CrossRef\]](#)
- Hamer OW, Aguirre DA, Casola G, et al. Fatty liver: imaging patterns and pitfalls. *Radiographics*. 2006;26(6):1637-1653. [\[CrossRef\]](#)
- Menesson N, Dumortier J, Hervieu V, et al. Liver steatosis quantification using magnetic resonance imaging: a prospective

- comparative study with liver biopsy. *J Comput Assist Tomogr*. 2009;33(5):672-677. [\[CrossRef\]](#)
- Poetter-Lang S, Bastati N, Messner A, et al. Quantification of liver function using gadoxetic acid-enhanced MRI. *Abdom Radiol (NY)*. 2020;45(11):3532-3544. [\[CrossRef\]](#)
- Wu Z, Matsui O, Kitao A, et al. Usefulness of Gd-EOB-DTPA-enhanced MR imaging in the evaluation of simple steatosis and nonalcoholic steatohepatitis. *J Magn Reson Imaging*. 2013;37(5):1137-1143. [\[CrossRef\]](#)
- Hojreh A, Lischka J, Tamandl D, et al. Relative enhancement in gadoxetate disodium-enhanced liver MRI as an imaging biomarker in the diagnosis of non-alcoholic fatty liver disease in pediatric obesity. *Nutrients*. 2023;15(3):558. [\[CrossRef\]](#)
- Verloh N, Probst U, Utpatel K, et al. Influence of hepatic fibrosis and inflammation: correlation between histopathological changes and Gd-EOB-DTPA-enhanced MR imaging. *PLoS One*. 2019;14(5):e0215752. [\[CrossRef\]](#)
- Ünal E, İdilman İS, Karaosmanoğlu AD, et al. Hyperintensity at fat spared area in steatotic liver on the hepatobiliary phase MRI. *Diagn Interv Radiol*. 2019;25(6):416-420. [\[CrossRef\]](#)
- Nguyen BD, Heller MT, Roarke MC. Nodular fat-sparing hepatic parenchyma as 11C-choline-avid finding on PET/CT. *Clin Nucl Med*. 2020;45(3):228-229. [\[CrossRef\]](#)
- Purandare NC, Rangarajan V, Rajnish A, Shah S, Arora A, Pathak S. Focal fat spared area in the liver masquerading as hepatic metastasis on F-18 FDG PET imaging. *Clin Nucl Med*. 2008;33(11):802-805. [\[CrossRef\]](#)
- Harisankar CN. Focal fat sparing of the liver: a nonmalignant cause of focal FDG uptake on FDG PET/CT. *Clin Nucl Med*. 2014;39(7):359-361. [\[CrossRef\]](#)
- Hod N, Levin D, Anconina R, et al. 68Ga-DOTATATE PET/CT in focal fatty sparing of the liver. *Clin Nucl Med*. 2019;44(10):815-817. [\[CrossRef\]](#)
- Smith EA, Salisbury S, Martin R, Towbin AJ. Incidence and etiology of new liver lesions in pediatric patients previously treated for malignancy. *AJR Am J Roentgenol*. 2012;199(1):186-191. [\[CrossRef\]](#)
- Vasireddi AK, Leo ME, Squires JH. Magnetic resonance imaging of pediatric liver tumors. *Pediatr Radiol*. 2022;52(2):177-188. [\[CrossRef\]](#)
- Özcan HN, Karçaaltıncaba M, Seber T, et al. Hepatocyte-specific contrast-enhanced MRI findings of focal nodular hyperplasia-like nodules in the liver following chemotherapy in pediatric cancer patients. *Diagn Interv Radiol*. 2020;26(4):370-376. [\[CrossRef\]](#)
- Schooler GR, Hull NC, Lee EY. Hepatobiliary MRI contrast agents: pattern recognition approach to pediatric focal hepatic lesions. *AJR Am J Roentgenol*. 2020;214(5):976-986. [\[CrossRef\]](#)